

Supporting Information

Synergistic Enhancement Effect of Ag/rGO as SERS Platform for Capture and Trace Detection of Fenvalerate Molecules

Minghui Yu^{1‡}, Chongyang Qin^{1‡}, Zhi Yu¹, Biao Sun³, Dejiang Ni¹, De Zhang^{1} and Pei Liang^{2,*}*

¹ National Key Laboratory for Germplasm Innovation and Utilization for Fruit and Vegetable Horticultural Crops, Key Laboratory of Horticultural Plant Biology, Ministry of Education, College of Horticulture & Forestry Sciences, Huazhong Agricultural University, 430070, Wuhan, China

² College of Optical and Electronic Technology, China Jiliang University, 310018 Hangzhou, China

³ School of Electrical and Information Engineering, Tianjin University, 300000, Tianjin, China

[‡] These authors contribute to this paper equally.

* zdybfq@163.com (D.Z.); plianghust@gmail.com (P.L.).

Material and Methods

Materials and Reagents

Silver nitrate (AgNO₃, ≥99.9% purity), ascorbic acid (ASA, ≥99.0% purity), polyvinylpyrrolidone (PVP, K30, >95% purity), and 4-aminobenzenethiol (4-ABT, ≥98% purity) were purchased from Aladdin Reagent Co., Ltd. (Shanghai, China); graphite powder and potassium permanganate (KMnO₄, ≥99.5%) from Sinopharm Chemical Reagent Co., Ltd. (Shanghai, China); concentrated sulfuric acid (H₂SO₄) and hydrogen peroxide solution (H₂O₂, 30%) from Huadong Pharmaceutical Co., Ltd. (Hangzhou, China); and hydrochloric acid (HCl, 1.18 g/mL) and absolute ethanol from Zhejiang Sanying Chemical Reagent company (Zhejiang, China). Ultrapure water (18.3 MΩ) obtained by UPH ULTRAPURE WATER SYSTEM (Chengdu super pure Technology Co., Ltd., China) was used to prepare all the aqueous solutions. All chemicals were of analytical grade and used without further purification.

Instruments

Material structural characterization was performed using field-emission scanning electron microscopy (HITACHI, SU8010, FE-SEM), field-emission high-resolution transmission electron microscopy (Thermo Fisher, Talos F200S, TEM), X-ray photoelectron spectroscopy (Thermo Fisher Scientific, XPS), and UV-vis spectroscopy (TU-1901, Purkinje, China). SERS spectra were collected using the Raman system (Horiba, LabRAM HR, Japan) at an excitation wavelength of 532, 633, and 785 nm. Ultrasonic vibration was performed using an ultrasonic oscillator (GEX750-5D, Saines Instruments Co., Ltd, USA), while ordinary dissolution was performed using the ultrasonic cleaning instrument (PS-20, Jiekang company, China). Stirring was implemented using a constant temperature magnetic stirrer (08-2G, Mei Yingbu, China). The centrifugal operation was completed using a table-top high-speed centrifuge (TG16-WS, Xiangyi, China). All the drying processes were conducted in the vacuum drying oven (DZF-6050, Shanghai Jinghong Experimental Equipment Co., Ltd, China).

Fabrication of Ag/rGO Hybrid Material

Graphene oxide (GO) was prepared using the improved classical Hummers method.¹ Briefly, 0.8 g of graphite powder was weighed into a beaker, followed by slowly adding 50 mL of concentrated sulfuric acid into the beaker under slow stirring with a glass rod and then 4 g of potassium permanganate with further stirring for 2 min. Next, the beaker was put in a magnetic stirrer for stirring at 1500 rpm for 4 h, followed by adding 4 mL of hydrogen peroxide solution and 100 mL of deionized water and then exposing the solution in the beaker to ultrasonic oscillation for 30 min. After separating it from the solution by centrifugation at 8000 rpm for 10 min, the reaction product was washed in 10 mL of deionized water and diluted hydrochloric acid (3%) in an ultrasonicator for 10 min to remove the impurities until solution pH 7. Finally, graphene oxide was dispersed in 20 mL of deionized water for further use.

The preparation of the Ag/rGO composite substrate was performed as follows: 1 mL of GO solution and 2 mL of ascorbic acid solution (0.5 M) were mixed thoroughly with 47 mL of deionized water in a triangular flask, followed by vibrating the mixed solution strongly using an ultrasonic oscillator with 70% amplitude at 60°C for 30 min and adding an amount of AgNO₃ solution (0.1 M) dropwise into the mixed solution under ultrasonic oscillation for 5 min. Next, the reaction product was separated from the solution by centrifugation at 12000 rpm for 10 min and then washed in 10 mL of a mixture of equal proportions of ethanol and deionized water in an ultrasonicator for 10 min. The above two steps were repeated four times to remove the impurities. Finally, the obtained Ag/rGO material was dispersed in 10 mL of deionized water for further analysis.

SEM, TEM, EDS, XPS, and Raman Analysis

For SEM, XPS, and EDS analyses, 2 mL of Ag/rGO colloid was pipetted on a Si wafer (0.5×0.5 cm), allowing the solution to immerse the whole Si wafer, followed by drying the treated Si wafers in a vacuum oven at 60 °C for 6 h to avoid oxidation. Finally, the Si wafer coated with Ag/rGO was used for SEM, XPS, and EDS characterization.

For TEM analysis, Ag/rGO colloid was pipetted on a copper mesh (0.5×0.5 cm), followed by drying in a vacuum oven at 60 °C for 6 h and then using the copper mesh coated with Ag/rGO for TEM characterization.

For AFM analysis, 30 μL of GO solution was pipetted on a Si wafer (0.5×0.5 cm), followed by drying the treated Si wafers in a vacuum oven at 60 °C for 6 h to avoid oxidation. Finally, the Si wafer coated with GO was used for AFM characterization.

SERS test of 4-ABT: the Si wafers coated with Ag/rGO were immersed in an aqueous solution of 4-ABT with gradient concentration (10^{-10} M- 10^{-2} M) for 1 h and then transferred into the vacuum oven at 40°C for 8 h. Finally, the dried samples were measured using Raman spectroscopy, and the SERS spectra of 4-ABT were acquired under a 532 nm laser at 25% power, with 5 s exposure time and two accumulations.

SERS test of fenvalerate: the Si wafers deposited with Ag/rGO were immersed in an aqueous solution of fenvalerate with gradient concentration (2.38×10^{-9} M- 2.38×10^{-5} M) for 1 h and then transferred into the vacuum oven at 40 °C for 8 h. Finally, the dried samples were measured using Raman spectroscopy, and the SERS spectra of fenvalerate were acquired under a 532 nm laser with 25% power, a 20 s exposure time, and one accumulation.

FDTD Simulation of Ag/rGO Material

For quantitative analysis of electromagnetic field intensity, FDTD calculation was performed using a code of FDTD Solution, which was developed by Lumerical Solutions for the accurate calculation of the electromagnetic field dispersion of a composite material by solving the Maxwell equations. The Ag/rGO was simulated as two Ag spheres, which were separated by different layers of graphene, and the mesh accuracy of the simulation field on the x, y, and z sides was $0.001 \times 0.001 \times 0.0001 \mu\text{m}$. The extinction spectra of Ag/rGO in the wavelength range of 250–800 nm were calculated under the conditions of a broadband total-field scattered-field source and perfectly matched layer (PML), with the thickness of each layer of graphene set at 0.34 nm. The local electromagnetic fields in the vicinity of Ag/rGO were simulated in terms of electric field (E2) under the excitation by the incident light at the given wavelengths, with the field distribution monitor perpendicular to the light irradiation direction (monitoring the distribution of electromagnetic field between two spheres) and 1000 fs simulation time (ensuring complete decay of electromagnetic field).

Vibrational spectrum calculation of fenvalerate

The vibrational spectrum calculation of fenvalerate was based on the DFT/B3LYP functional and 6-31G(d,p) basis set via Gaussian 09, which was the same as the ground state geometric optimization². The IR peak half-width at half-height was set at 4 cm^{-1} . By using the frequency/intensity data from the B3LYP vibrational analysis as a sum of Lorentzian line shapes of 4 cm^{-1} half-width, the Raman spectrum was acquired, and the vibrational spectrum (frequencies) was corrected by a constant factor of 0.97 to align the Raman features with experimental results.

Theoretical modeling

The rGO and the fenvalerate molecules were explored by using density functional theory (DFT) with the hybrid B3LYP functional based on the Gaussian 09 computational package. The 6–31 G (d, p) basis set was adopted to complete all the calculations. Geometries were reoptimized to explain the interaction of fenvalerate molecules and rGO, and an aperiodic structure with Gamma k-point was used to calculate both fenvalerate molecules and rGO^{3,4}.

Spectral data processing

All the raw SERS spectral baseline and noise were processed by wavelet transform algorithm through the Python program, using the Daubechies function for baseline correction and the heuristic threshold method for noise elimination, with a wavelet coefficient of db8 and a decomposition level of seven.

The LOD calculation details

We calculated the LOD of fenvalerate by using the following equation (S1)⁵ and its corresponding calibration plot (In equation (S1), $k=3$ allowed for a confidence level of 98.9%). Three SERS parallel tests were performed on blank samples, and the mean SERS intensity (IB) and standard deviation (SB) were obtained.

$$I_L = I_B + k \times S_B \quad (\text{S1})$$

In this equation, I_L represents the minimum SERS signal intensity that can be detected, and I_B represents the average SERS intensity of the blank sample. S_B represents the standard deviation, and k is a numerical factor chosen according to the desired confidence level. Based on the linear regression equation $y = -5.82x + 21.22$ ($R^2 = 99.2\%$), the LOD could be calculated as 1.69×10^{-5} mg/kg, which is far lower than the relevant residue standard (European Union: 0.02 mg/kg; China: 2 mg/kg).

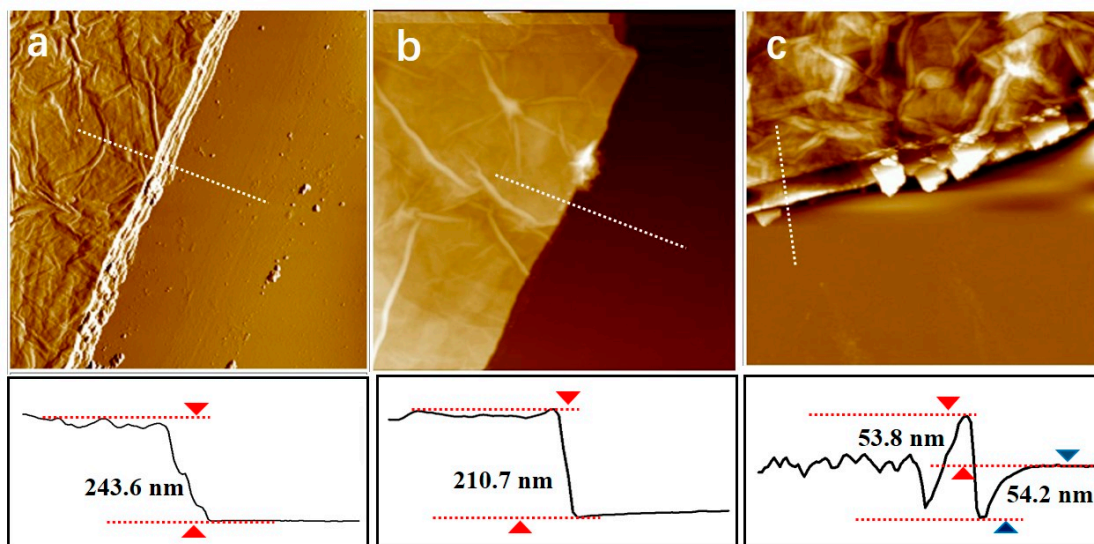


Figure S1. The AFM images of the different positions of graphene oxide.

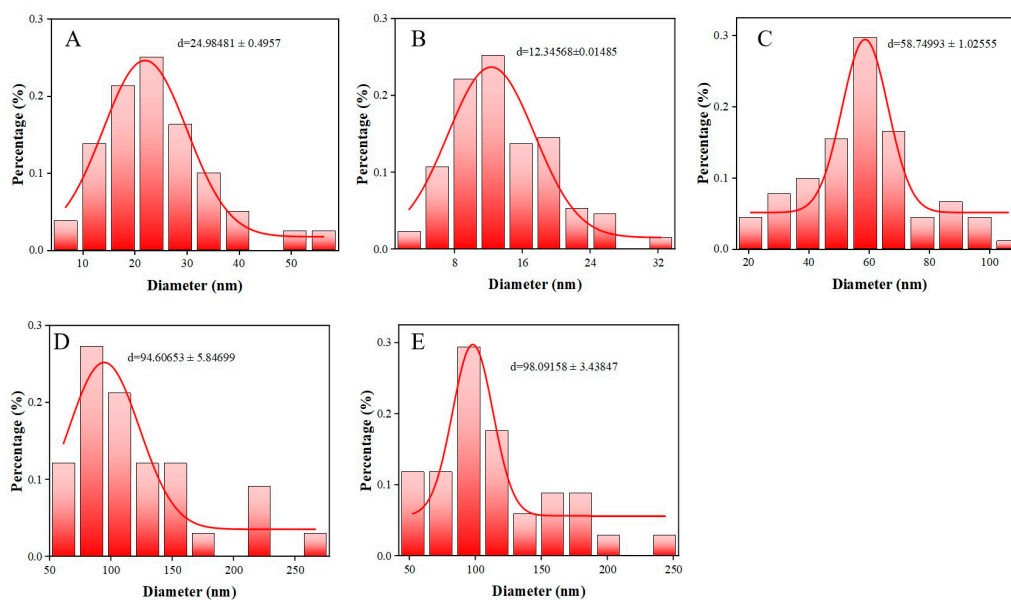


Figure S2. Particle distribution of Ag NPs in each AgNO_3 concentration.

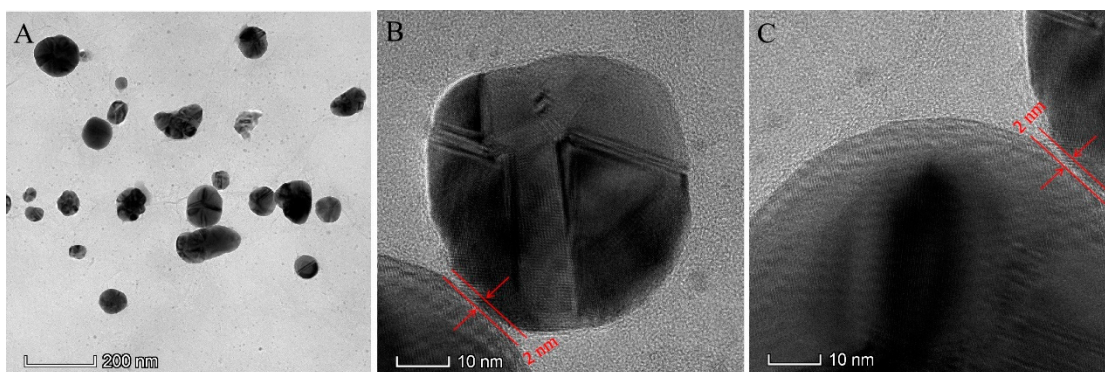


Figure S3. The TEM images of Ag/rGO material.

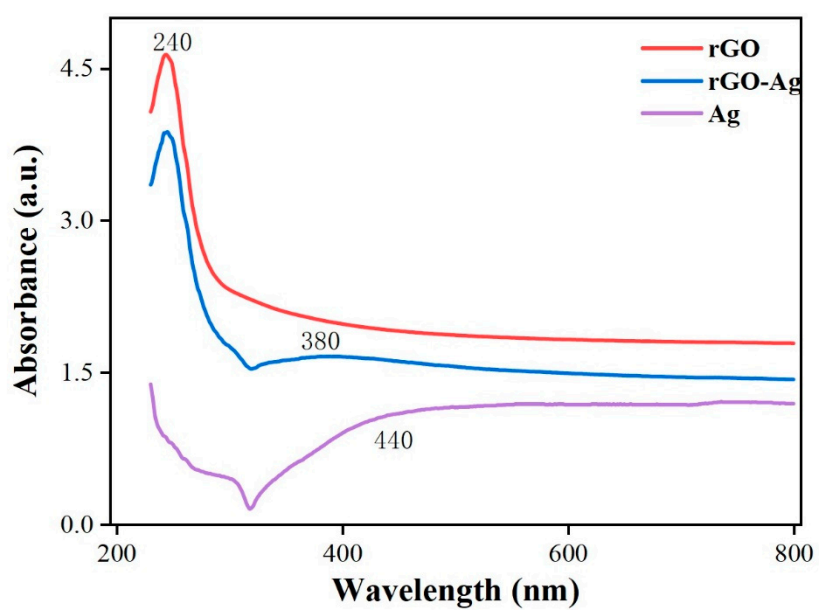


Figure S4. UV-vis spectra of pure Ag, rGO, and Ag/rGO.

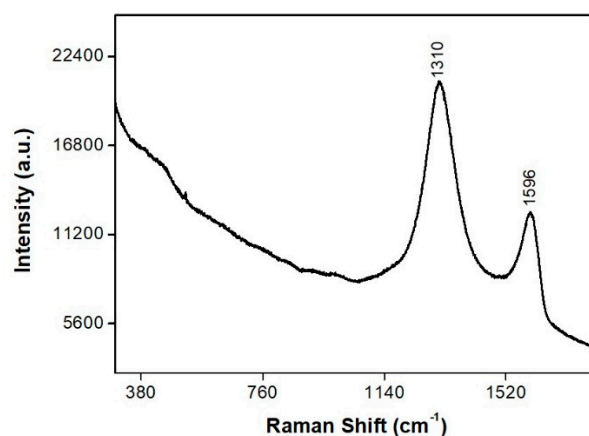


Figure S5. The Raman spectra of 4-ABT based on rGO

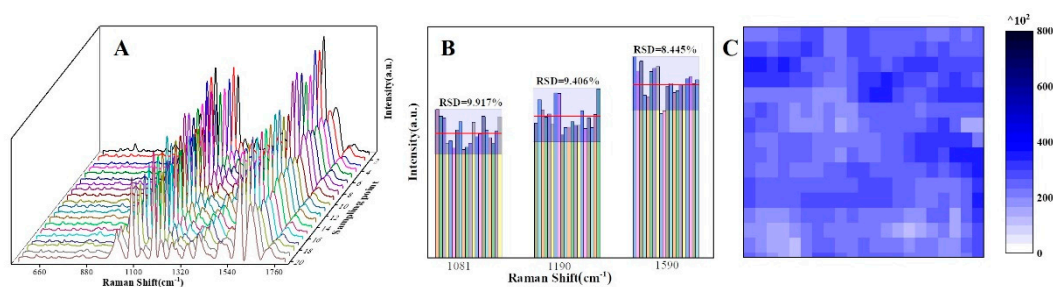


Figure S6. SERS spectra statistical diagram of 4-aminothiophenol (10^{-4} M) obtained from 20 randomly selected points on Ag/rGO substrate (A); statistical diagram of the Raman signal intensity at 1081, 1190, and 1590 cm^{-1} (B); SERS mapping of 4-aminothiophenol (10^{-4} M) obtained at 1139 cm^{-1} based on Ag/rGO substrate (C).

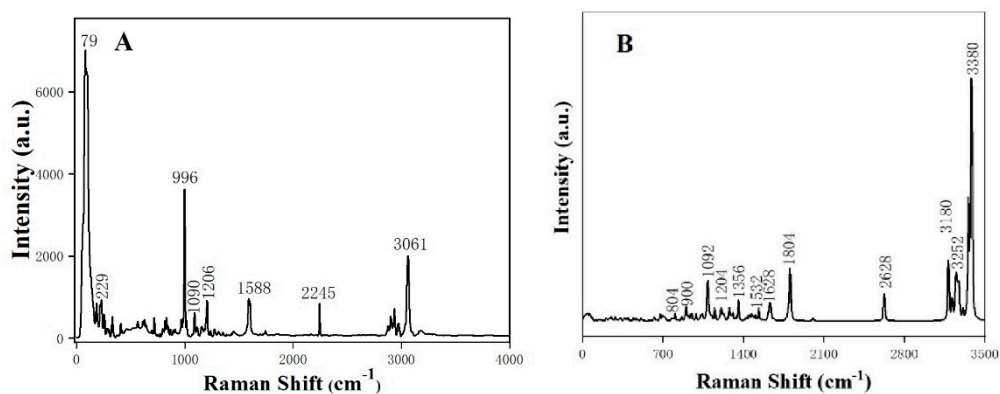


Figure S7. Normal Raman of fenvalerate solid powder (A) and Raman of fenvalerate obtained using DFT calculation (B).

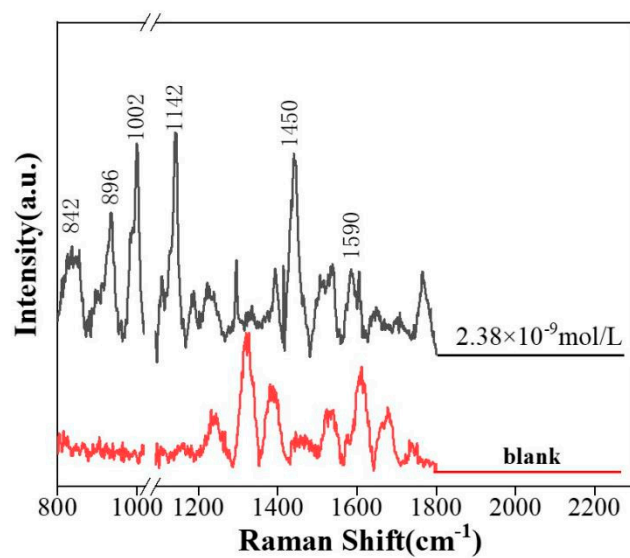


Figure S8. SERS spectra of fenvalerate (2.38×10^{-9} M) (A) and blank composite substrate (B).

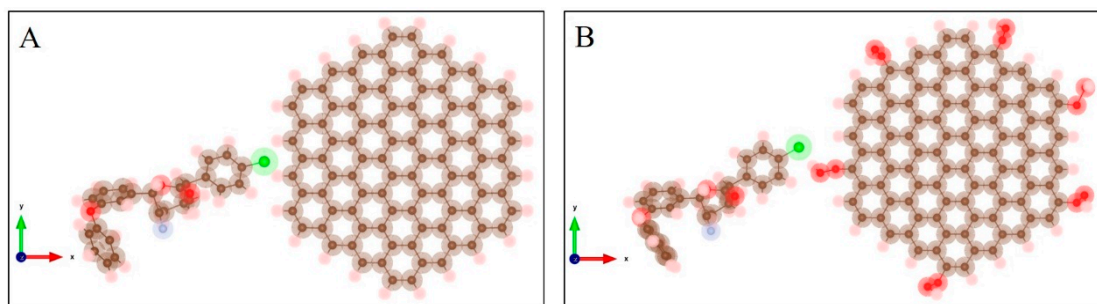


Figure S9. The interaction model between rGO and fenvalerate: H group (A) and COOH (B).

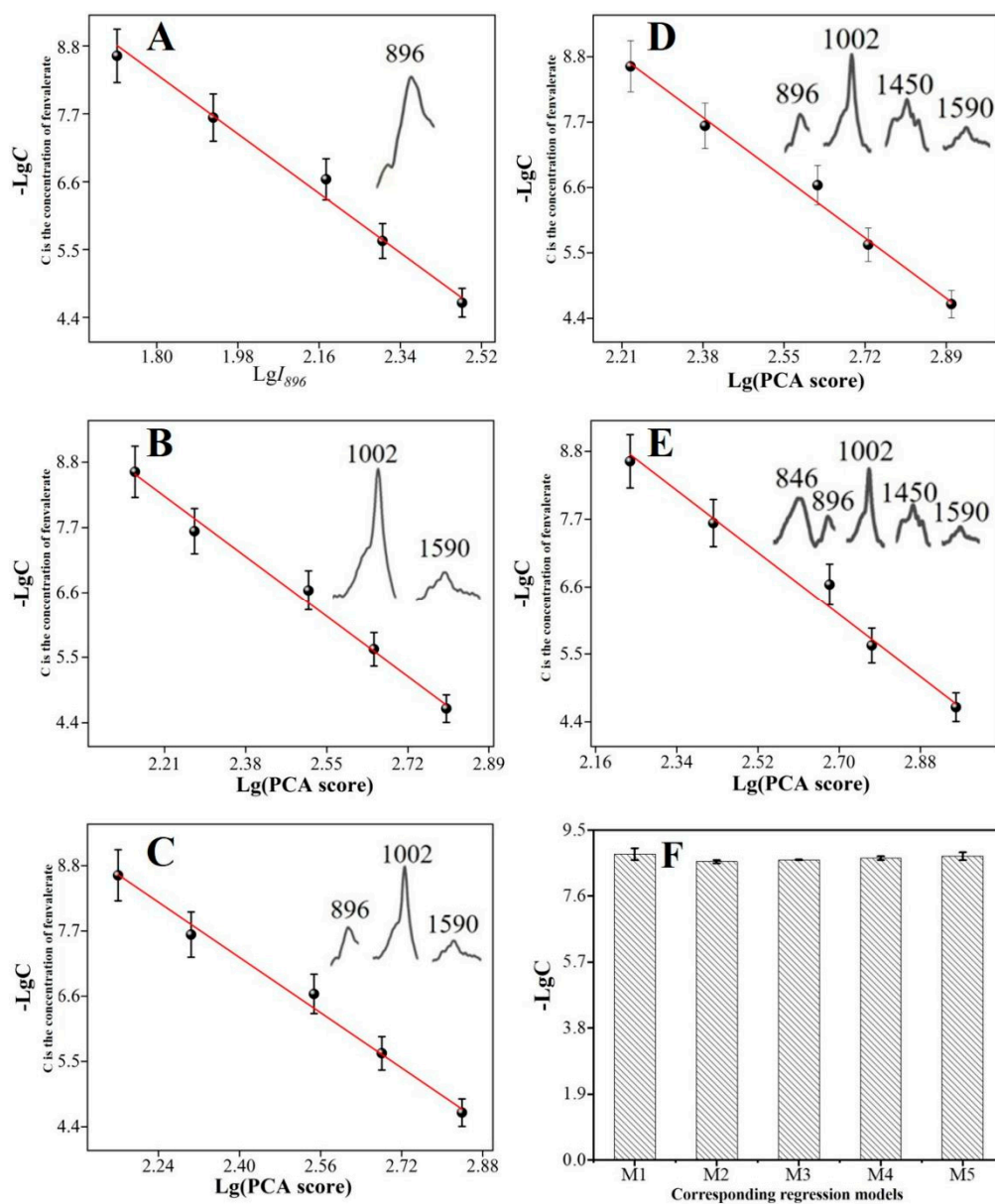


Figure S10. The linear regression of fenvaletrate with different characteristic peaks: single peak (A), two peaks (B), three peaks (C), four peaks (D), and five peaks (E), and the error verification of $-\text{Lg}C$ was conducted with different relevant equations when the concentration of fenvaletrate was $2.38 \times 10^{-8} \text{ M}$ (F).

Table S1. The SERS performance comparison of the substrate between this paper and others.

| Substrate | Synthetic method | Probe molecule | Sensitivity | Ref |
|---------------------------------------|---|----------------|---------------------|------------|
| Fe ₃ O ₄ /GO/Ag | Solvothermal reaction-APTES modification-in situ deposition | Methylene blue | 10 ⁻⁹ M | 6 |
| AgNFs/GO/AuNS | Liquid phase reduction- seed-mediated growth-assembling | R6G | 10 ⁻¹³ M | 7 |
| Au@Ag NPs/GO/Au@Ag NP | Si modification-assembling-PEI-GO coated | R6G | 10 ⁻⁷ M | 8 |
| AgNPs/CNT-GO | Seded-growth- PDDA-functionalized CNTs-GO- filter | R6G | 10 ⁻¹³ M | 9 |
| GO/Ag | Liquid phase reduction | R6G | 10 ⁻⁹ M | 1 |
| GO/AuNPs | Liquid phase reduction | Mlachite green | 10 ⁻⁴ M | 10 |
| Ag/rGO | Liquid phase reduction | 4-ABT | 10 ⁻¹⁰ M | This paper |

Table S2. Variance contribution rate and cumulative variance contribution rate of PCA linear fitting of two Raman peaks.

| Component and Raman frequency (cm ⁻¹) | Initial Eigenvalues | | | Extraction Sums of Squared Loadings | | |
|---|---------------------|--------------|----------------|-------------------------------------|--------------|----------------|
| | Total | Variance (%) | Cumulative (%) | Total | Variance (%) | Cumulative (%) |
| 1 (1002) | 1.9264 | 96.32 | 96.32 | 1.9264 | 96.32 | 96.32 |
| 2 (1590) | 0.0736 | 3.68 | 100.00 | | | |

Table S3. Variance contribution rate and cumulative variance contribution rate of PCA linear fitting of three Raman peaks.

| Component and Raman frequency (cm ⁻¹) | Initial Eigenvalues | | | Extraction Sums of Squared Loadings | | |
|---|---------------------|--------------|----------------|-------------------------------------|--------------|----------------|
| | Total | Variance (%) | Cumulative (%) | Total | Variance (%) | Cumulative (%) |
| 1 (896) | 2.9180 | 97.27 | 97.27 | 2.9180 | 97.27 | 97.27 |
| 2 (1002) | 0.0804 | 2.68 | 99.95 | | | |
| 3 (1590) | 0.0015 | 0.05 | 100.00 | | | |

Table S4. Variance contribution rate and cumulative variance contribution rate of PCA linear fitting of four Raman peaks.

| Component and Raman frequency (cm ⁻¹) | Initial Eigenvalues | | | Extraction Sums of Squared Loadings | | |
|---|---------------------|--------------|----------------|-------------------------------------|--------------|----------------|
| | Total | Variance (%) | Cumulative (%) | Total | Variance (%) | Cumulative (%) |
| 1 (896) | 3.8803 | 97.01 | 97.01 | 3.8803 | 97.01 | 97.01 |
| 2 (1002) | 0.1021 | 2.55 | 99.56 | | | |
| 3 (1449) | 0.0174 | 0.43 | 100.00 | | | |
| 4 (1590) | 0.0001 | 0.00 | 100.00 | | | |

Table S5. Variance contribution rate and cumulative variance contribution rate of PCA linear fitting of five Raman peaks.

| Component and Raman frequency (cm ⁻¹) | Initial Eigenvalues | | | Extraction Sums of Squared Loadings | | |
|---|---------------------|--------------|----------------|-------------------------------------|--------------|----------------|
| | Total | Variance (%) | Cumulative (%) | Total | Variance (%) | Cumulative (%) |
| 1 (846) | 4.8653 | 97.31 | 97.31 | 4.8653 | 97.31 | 97.31 |
| 2 (896) | 0.1153 | 2.31 | 99.61 | | | |
| 3 (1002) | 0.0185 | 0.37 | 99.98 | | | |
| 4 (1449) | 0.0010 | 0.02 | 100.00 | | | |
| 5 (1590) | 0.0000 | 0.00 | 100.00 | | | |

1. Zheng, H.J.; Ni, D.J.; Yu, Z.; Liang, P. *Food Chemistry*, 2017, 217, 511-516.
2. Grimme, S. *Journal of Computational Chemistry*, 2006, 27, 1787-1799.
3. Delley, B. *The Journal of chemical physics*, 2000, 113, 7756-7764.
4. Delley, B. *Journal of Chemical Physics*, 1990, 92, 508-517.
5. Shrivastava, A.; Gupta, V.B. *Chron. Young Sci*, 2011, 2, 21-25.
6. He, J.; Song, G.; Wang, X.; Zhou, L.; Li, J. *Journal of Alloys and Compounds*, 2022, 893.
7. Zhang, C.-Y.; Zhao, B.-C.; Hao, R.; Wang, Z.; Hao, Y.-W.; Zhao, B.; Liu, Y.-Q. *Journal of Hazardous Materials*, 2020, 385.
8. Zhang, L.; Jiang, C.; Zhang, Z. *Nanoscale*, 2013, 5, 3773-3779.
9. Qu, L.-L.; Liu, Y.-Y.; Liu, M.-K.; Yang, G.-H.; Li, D.-W.; Li, H.-T. *ACS Appl. Mater. Interfaces*, 2016, 8, 28180-28186.
10. Fu, W.L.; Zhen, S.J.; Huang, C.Z. *Analyst*, 2013, 138, 3075-3081.